ISSN 2989-0705 (Online)|Vol 1|Issue 1|July 2023

Journal of Applied Learning | BMS make learning happen

One pot Biological Synthesis of Silver Nanoparticles using *Dracaena* Plant Leaf Varieties and assessing their Antioxidant, Photocatalytic, Antimicrobial Properties, and Melamine Adulteration.

Sachindya Linoli Bandaranayake[1], Ominda Perera[1] and Mathivathani Kandiah[1*]

[1]School of Science, Business Management School (BMS), Sri Lanka

*mathi@bms.ac.lk

Abstract

Nanotechnology, which is a result of a multidisciplinary research concept is a general term that refers to all advanced technologies in the field of working with nanoscale. Energy storage, optical engineering, biotechnology, biomedical and drug delivery are some of the applications of nanotechnology. In this study, Silver Nanoparticles (AgNPs) were synthesized using *Dracaena* leaf varieties such as *Dracaena sanderiana, Dracaena reflexa, Dracaena warnecki, Dracaena reflexa 'variegata',* and *Dracaena surculosa*. Scanning Electron Microscopic (SEM) analysis confirmed that the synthesized Nanoparticles (NPs) are spherical in shape and about 50 nm in size. These AgNPs were used to assess their antioxidant, photocatalytic, antimicrobial properties, and melamine adulteration. Phytochemical analysis was carried out for each water extract (WE) and the total flavonoid content (TFC), total phenolic content (TPC), and total antioxidant capacity (TAC) were measured using both WEs and synthesized nanoparticles. AgNPs showed higher TFC, TPC, and TAC compared to WEs. The DPPH radical scavenging assay revealed that the AgNPs have the higher DPPH percentage activity compared to the WEs. The photocatalytic activity was measured using both 267ppm, and 4000ppm AgNPs with Malachite green as the model dye. The dye degraded faster after the addition of $NaBH_4$. Five melamine concentrations were used to detect melamine using DRE AgNPs and Melamine was detected in 2mM solution. *Staphylococcus aureas* and *Escherichia coli* strains were used to determine the antibacterial activity of AgNPs. AgNPs showed higher Zone of inhibition (ZOI) compared to the WE. However, this study confirms the vast number of properties of synthesized nanoparticles such as drug delivery, radiosensitivity treatments, and for diagnosis of the diseases like CVD, and cancer.

Keywords: Silver Nanoparticles, *Dracaena*, Antioxidants, DPPH, Melamine.

1. Introduction

Nanotechnology is a result of a multidisciplinary research concept that was performed during the past few years. Further, it is a general term that refers to all advanced technologies in the field of working with nanoscale.[1] Usually, the purpose of nanoscale dimension is about 1 nm to 100 nm (Figure 1). Nanotechnology is a fast-growing technology that can synthesize nanoparticles using numerous systems and their applications (Figure 2). In this research, the silver nanoparticles were synthesized using *Dracaena* plant leaf varieties. Silver is chosen to synthesize AgNPs over other metals due to their unique physical and chemical properties such as optical, electrical, and thermal, high electrical conductivity, and biological properties.[2] There are two basic methods for synthesizing nanoparticles: top-down and bottom-up (figure 3). Breaking down the bulk material into nano-sized structures or particles is a top-down approach. The bottom-up approach is also intended when nanoparticles are created through chemical reactions between atoms, ions, and

molecules. In the bottom-up approach, different techniques can be used to synthesize nanoparticles: physical, chemical, and biological.

6

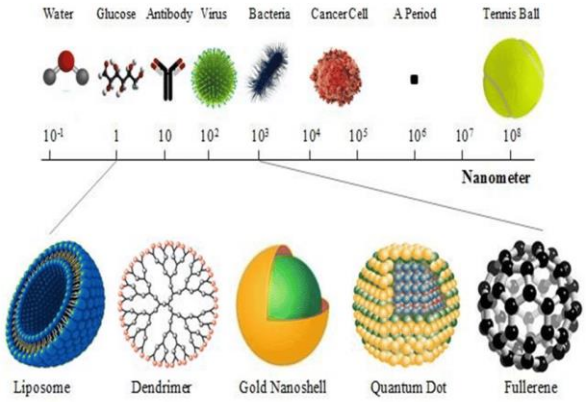

Figure 1. Nanoscale.[3]

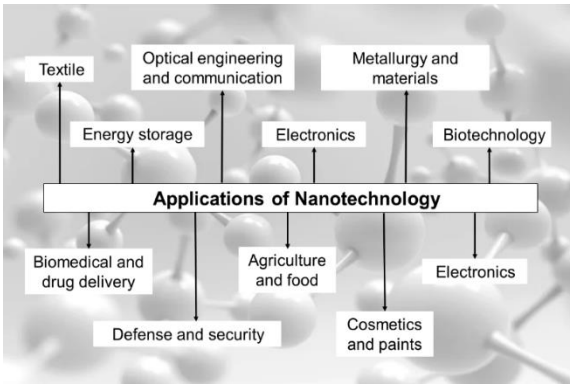

Figure 2. Applications of Nanotechnology.[4]

There are two basic methods for synthesizing nanoparticles: top-down and bottom-up (figure 03). Breaking down the bulk material into nano-sized structures or particles is a top-down approach. The bottom-up approach is also intended when nanoparticles are created through chemical reactions between atoms, ions, and molecules. In the bottom-up approach, different techniques can be used to synthesize nanoparticles: physical, chemical, and biological.[6] The physical method consists of two approaches such as evaporation condensation and laser ablation which are responsible for the production of nanoparticles in high

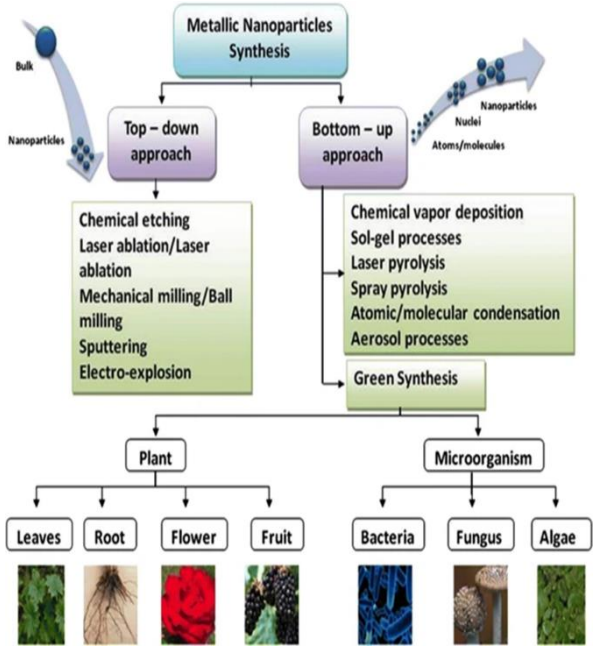

Figure 3. Metallic Nanoparticle Synthesis.[5]

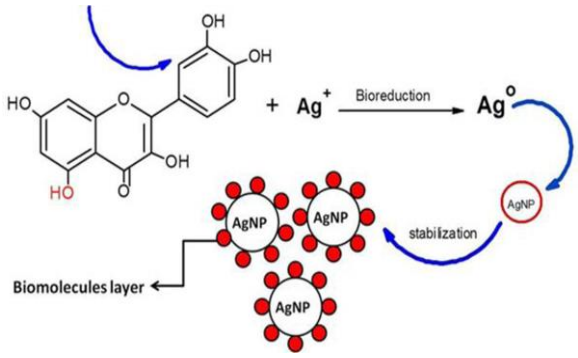

Figure 4. Nanoparticle Synthesis Mechanism.[9]

concentration. In the chemical method, different reducing agents (such as sodium citrate) are used to reduce Ag^{+} in solutions both aqueous and nonaqueous [7]. The biological method refers to microorganisms, bio-templates, and plant extracts-assisted biogenesis. [8] In comparison to other biological processes, plants are the finest synthesizers due to the vast availability of resources. Additionally, the presence of nontoxic compounds in plants offers a better platform for the synthesis of AgNPs.

Plants also lower the cost of improving culture medium and isolating microorganisms. In green synthesis, the phytochemicals (proteins, flavonoids, phenols, and enzymes) act as capping agents to stabilize the silver nanoparticles (Figure 4). The sample selected for the research was *Dracaena* which is an indoor plant native to the old-world tropics, Africa, southern Asia, and northern Australia (Figure 5). It has about 120 species. *Dracaena* is a good air purifier, increases concentration and sharpens focus, increases humidity, low maintenance, and absorbs lead. Furthermore, they contain numerous antioxidants [10]. Five varieties of dracaena leaf were collected from Henarathgoda Botanical Gardens, Gampaha, Sri Lanka for this research.

As mentioned above, these Dracaena plants contain numerous antioxidants such as phenols and flavonoids. Antioxidants are molecules, either natural or artificial, that can stop, or delay cell damage brought on by oxidants like Reactive Oxygen Species (ROS), Reactive Nitrogen Species (RNS), free radicals, and other unstable molecules.[11] An atom with an unfilled outer shell (a free radical) is unstable and reacts with other substances fast to balance out the number of electrons in the outer shell. When oxygen

Figure 5. Dracaena Plant.[14]

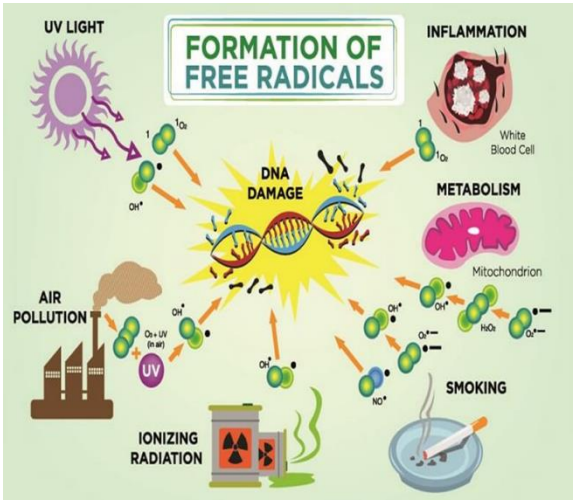

Figure 6. Formation of free radicals.[11]

molecules break into single unpaired electron atoms, the resulting free radicals are unstable and seek out other atoms or molecules to form bonds with (Figure 6). As a result, oxidative stress starts to occur. Free radicals are neutralized by antioxidants.[12] Thus, antioxidants serve as scavengers (Figure 7). Adverse effects of synthetic antioxidants may cause DNA damage,[13] hence interest in natural antioxidants with plant origins is growing.

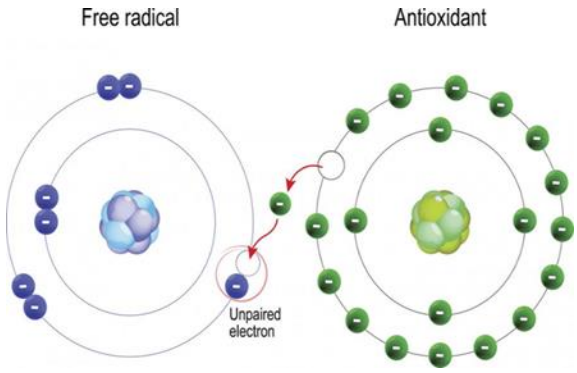

Figure 7. Antioxidant defense mechanism.[12]

DPPH can be used to determine whether many strategies for lowering pollution levels and is regarded as a very effective, environmentally antioxidants are stabilized in a sample that is rich in antioxidants. It is based on the evaluation of antioxidants' ability to scavenge it.[15]

AgNPs release Ag^+ ions during their antibacterial activity, which can build up on the cell walls and membranes of microorganisms and then move into their cytoplasm. Reactive Oxygen Species (ROS), which are the primary cause of antimicrobial activity and which are produced inside of cells by Ag^+ ions, include (1) inhibition of DNA synthesis, (2) inhibition of mRNA synthesis, (3) destruction of cell membranes and leakage of cell components, (4) inhibition of protein synthesis, (5) inhibition of cell-wall synthesis, (6) mitochondrial damage, and (7) inhibition of the electron transport chain (Figure 08). Cell death is the result of these effects. Thus, AgNPs can destroy bacteria.[16]

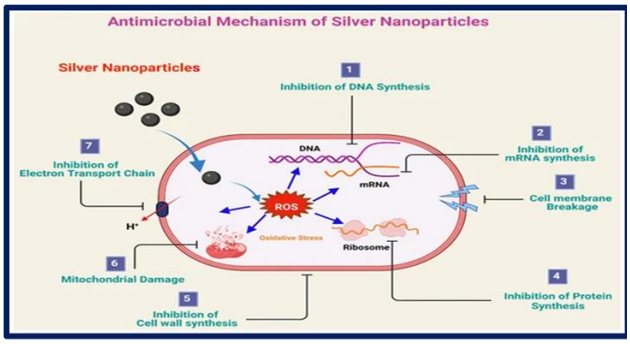

Figure 08: Antibacterial mechanism of silver nanoparticles [16].

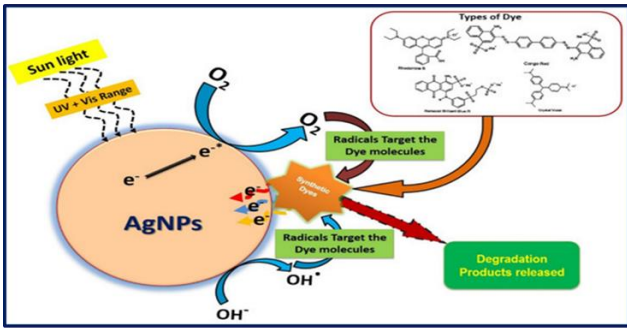

Figure 09: Photocatalytic mechanism [19]

Photocatalysts are regarded as a green method of cleaning the environment and play a critical part in the degradation of contaminants in the environment. Photocatalytic activity is one of many strategies for lowering pollution levels and is regarded as a very effective, environmentally friendly, and economical strategy.[17] Due to the visible and UV regions of the solar spectrum (due to surface plasmon resonance) and inter-band transition properties of AgNPs, they are used as photocatalysts.[18] During the photocatalytic activity, valence band electrons absorb energy from sunlight and then get excited into the conduction band. These electrons are involved in the formation of free radicals from molecules like water and oxygen. Free radicals will attack azo bonds in the synthetic azo dyes causing the degradation of compounds forming colorless solutions (Figure 9).[19]

Melamine is a chemical that is high in Nitrogen content. It gives rise to the conditions such as uric acid stones.[20] When submitted to a test for protein levels that is based on nitrogen content, melamine gives the impression that normal protein levels have been added to diluted milk. The silver nanoparticles become aggregated when melamine is added to them.[21] Due to their lower cost, safer by products and better extinction coefficient, AgNPs are more frequently used in the detection of different analytes than conventional methods.[22]

The principle objectives of this research are to synthesize silver nanoparticles using five species of *Dracaena* plant leaf and to determine their morphology by SEM analysis, evaluate antioxidant properties using total flavonoid content (TFC), total phenolic content (TPC), total antioxidant capacity (TAC), DPPH radical scavenging assay, and photocatalytic activity using Malachite green dye, antimicrobial properties using *Escherichia coli* and *Staphylococcus aureus* and melamine adulteration in milk using silver nanoparticles. After achieving the objectives of this study, AgNPs can be an effective method for treating diseases caused by free radicals, and creating an environment free of toxic substances like azo dyes.

2. Methodology

2.1. Extraction of Dracaena leaves using water. The leaves were cleaned with tissue paper to remove dust and impurities. The cleaned leaves were shade dried on different trays with labels without exposing them to direct sunlight. After a few days, the leaves were kept inside the oven at 40ºC to dry in the lab. The dried leaves were finely cut, and 2 g of each sample was weighed and placed in different beakers. 50 mL of distilled water was added, and the beakers were covered with Al foil. The beakers were placed in the oven at 80ºC for 20 minutes. The boiled aqueous solutions were left to cool down and the extracts were separated by filtration using Whatman No.1 filter papers. They were stored at 4ºC until further use.

2.2. Sample Collection. Dracaena leaf varieties were collected from the Botanical Garden, Gampaha, Sri Lanka (Figure 10)

Figure 10: Samples collected for the research (A. Dracaena sanderiana - DSA, B. Dracaena reflexa - DRE, C. Dracaena warnecki - DWA, D. Dracaena reflexa 'variegata' - DRV, E. Dracaena surculosa - DSU).

Table 2. Test, methodology, and expected result of phytochemical analysis.[23]

Test	Procedure
Test for Proteins	0.5 mL of each extract was added to 5 test tubes separately and a few drops of Millons reagent were added to them.
Test for Carbohydrates	0.5 mL of each extract was added to 5 test tubes separately. 2 drops of Molisch reagent were added to them and conc. H_2SO_4 was added along the wall.
Test for Saponins	2 mL of distilled water was added to the test tubes along with the extracts (0.5 mL) and they were shaken vigorously.
Test for Tannins	A few drops of 2% $FeCl_3$ were added to the test tubes containing the extracts (0.5 mL).
Test for Flavonoids	A few drops of NaOH were added to the test tubes containing the extracts (0.5 mL). Few drops of dil. H_2SO_4 were added to them.
Test for Steroids	1.5 mL chloroform were added to the test tubes containing extracts (0.5 mL) and 1.5 mL 0f H_2SO_4 were added to them.
Test for Anthraquinone glycoside	A volume of 1 mL ammonia was mixed with extracts (0.5 mL) and the mixtures were shaken vigorously.
Test for Phenols	To the 1 mL of the filtrates, a few drops of $FeCl_3$ were added.

2.3. Qualitative Analysis of Phytochemicals. Phytochemical tests were performed on 0.5 mLof each extract following the procedure in table 02.

2.4. Synthesis of Silver Nanoparticles (AgNPs). 1 mM aqueous $AgNO_3$ solution was prepared. Next, 1 mL of each extract and 9 mL of $AgNO_3$ solution were added into test tubes separately and covered with Al foil. One from each sample (from prepared solutions) was kept at 90ºC and 60ºC for 15-minute intervals until 1 hour. Another set of samples was kept at room temperature for 24 hours. The absorbance was measured from 320nm to 520nm and distilled water was used as the blank.

2.5. SEM Analysis. 1 mL of DRE AgNPs was diluted with 2 mL of distilled water. It was centrifuged at 13,000rpm for 3 minutes. It was repeated until the pellet occurs. Then the supernatant was discarded, and the rest was kept drying. After that, it was sent for SEM analysis at the Institute of Nanotechnology (SLINTEC).

2.6. Quantitative Analysis of Phytochemicals. Water extracts and AgNPs were diluted 15 times and used for the following Quantitative analysis.

2.6.1. Determination of Total Flavonoid Content (TFC). 2 mL of sample was mixed with 0.1 mL of 10% aluminum chloride hexahydrate, 0.1% mL of 1M potassium acetate. After 40 minutes of incubation at room temperature, the absorbance of the reaction mixture was determined spectrophotometrically at 415nm. The determination of total flavonoids in the extracts and AgNPs was carried out in triplicates. Distilled water was used as the blank. Results were expressed in µg Quercetin equivalents per 100 g (µg QE/100 g).[10]

*2.6.2. Determination of Total Phenolic Content (TPC).*0.5 mL of the sample was mixed with 1.25 mL of 10% Folin-Ciocalteau phenol reagent. After 5 minutes, 2 mL of 7.5% Na_2CO_3 solution was added to each tube, and they were incubated in the dark for 90 minutes at room temperature after fully covering them with foil paper. The absorbance of the extracts and AgNPs was measured at 750nm with a UV visible spectrometer. The determination of TPC was carried out in triplicates. Distilled water was used as the blank. Results were expressed in g gallic acid equivalents per 100 g (g GAE/100 g).[10]

2.6.3. Determination of Total Antioxidant Capacity (TAC). 1 mL of extracts and AgNPs at 90ºC for 15 minutes were added to the tubes and 3 mL of reagent solution (0.6M Sulfuric acid, 28Mm Sodium phosphate and 4Mm Ammonium molybdate in 1:1:1 ratio) was added to them. Solutions were incubated at 95ºC for 90 minutes. The absorbance of the reaction mixtures was measured at 695nm using a spectrometer. TAC was determined using triplicates. Distilled water was used as the blank. Results were expressed as g ascorbic acid equivalents per 100 g (g AAE/ 100 g).[10]

*2.6.4. 2,2-Diphenyl-1-picrylhydrazyl (DPPH) Scavenging Activity.*2 mL of 0.1 mM DPPH were added to 1 mL of the samples. They were kept in dark for 20 minutes. After that, the absorbance was measured at 517nm and the %DPPH scavenging activity was calculated using the bellow equation (Figure 11). Methanol was used as the blank.[10]

$$\%DPPH = A(control) - \frac{A(sample)}{A(control)} \times 100$$

Figure 11. Equation for %DPPH radical scavenging activity.

2.7. Melamine Detection. Melamine detection was carried out according to the following methods.

2.7.1. Melamine Detection using DRE AgNPs. Melamine solutions were made with different concentrations (1 mM, 2 mM, 4 mM, 6 mM and 8 mM). 500 µL of AgNPs were added to the test tubes. 300 µL of melamine were added to them. After that, the tubes were kept for 5 minutes. The absorbance was measured from 320nm to 700nm for 10-minute intervals until 40 minutes. Distilled water was used as the blank.

2.7.2. Melamine Detection on Spike Milk. The milk sample was pre-treated with 300 g/L trichloroacetic acid and the mixture was vortexed

until a white precipitate was observed. The mixture was filtrated using Whatman No.1 filter paper. The pH of the filtrate was adjusted to 7.0 by adding 3 M NaOH. It was converted into 2 different samples such as milk without melamine (control) and milk with melamine (1 mM). Lastly, the absorbance was measured for 30-minute intervals until 1 hour from 320nm to 700nm after adding AgNPs. Distilled water was used as the blank.

2.8. Photocatalytic Activity. 450 µL of Malachite Green was added to 100 mL of distilled water. The absorbance was measured from 320nm to 800nm. Following which, 267ppm of AgNPs were added and the absorbance was measured from 320nm to 800nm for 30-minute intervals until 150 minutes. This was carried for 4000ppm AgNPs also. After that, $NaBH_4$ was added and the absorbance was measured from 320nm to 800nm for 5-minute intervals until 15 minutes. Distilled water was used as the blank. This was carried out with both 267ppm and 4000ppm AgNPs.

2.9 Antimicrobial Activity. The Kirby-Bauer method was carried out. *Staphylococcus aureus* and *Escherichia coli* bacterial cultures were evenly spread on the MHA plates. Three wells were created on the MHA (negative control, sample 1, sample 2) plates (Figure 12). Saline was added as the negative control (1 mL) and a gentamycin disc was added as the positive control. 1 mL of the sample was added to S_1 and S_2. The plates were incubated at 37ºC for 24 hours and the diameter of the zone of inhibition was measured in cm.

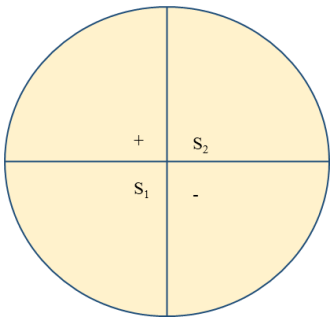

Figure 12. Petri plate labeling

2.10. Statistical Analysis. The one-way ANOVA statistical analysis was done using Microsoft® Excel 2016 software and the correlation coefficient was analyzed using IBM SPSS Statistics software.

3. Results

3.1. Phytochemical Analysis. The existence of phytochemicals in the *Dracaena* samples was revealed by phytochemical analysis as shown in Table 3.

As shown in the above-mentioned table, all the samples showed positive results for proteins, carbohydrates, saponins, tannins, phenols, flavonoids, and steroids except for anthraquinone glycoside.

3.2. Synthesis of AgNPs

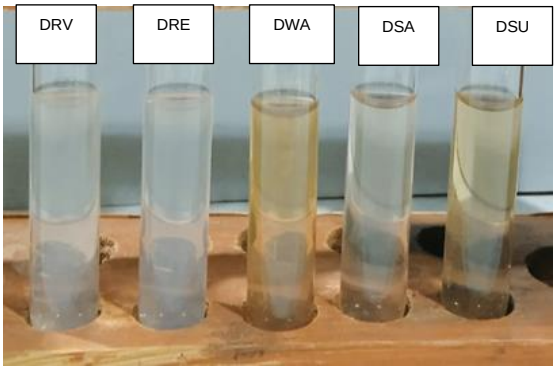

Figure 13. Before Synthesis AgNPs.

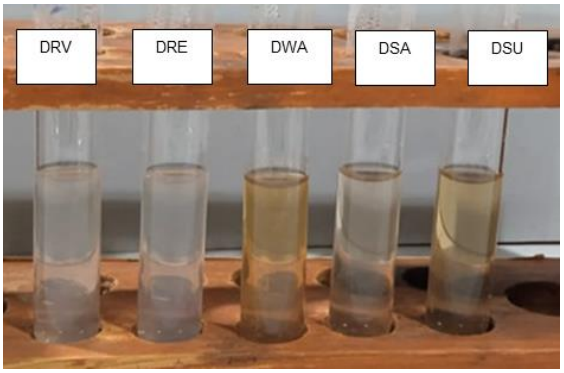

Figure 14. After Synthesis of AgNPs

A darker color was observed from the samples after the synthesis of AgNPs and the optimized sample's conditions were 90ºC for 15minutes.

Table 3. Phytochemical analysis for *Dracaena* water extracts.

Test	*Dracaena sanderiana*	*Dracaena surculosa*	*Dracaena reflexa*	*Dracaena reflexa 'variegate'*	*Dracaena warneckii*
Test for Proteins	+	+	+	+	+
Test for Carbohydrates	+	+	+	+	+
Test for Saponins	+	+	+	+	+
Test for Tannins	+	+	+	+	+
Test for Phenols	+	+	+	+	+
Test for Flavonoids	+	+	+	+	+
Test for Steroids	+	+	+	+	+
Test for Anthraquinone glycoside	-	-	-	-	-

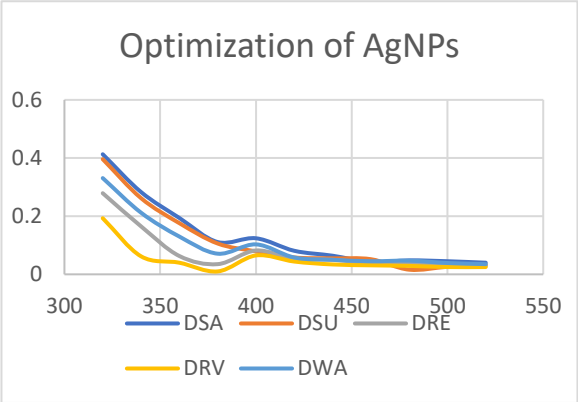

Figure 15. Optimization of AgNPs.

Table 4. Optimization Table

Temperature and Time		DSA	DSU	DRE	DRV	DWA
60ºC	15min	-	+	+	+	-
	30min	+	+	-	+	+
	45min	-	-	-	+	+
	60min	-	-	+	+	+
90ºC	15min	+	-	+	+	+
	30min	+	+	+	-	+
	45min	-	+	+	+	-
	60min	-	-	-	-	-
RT	24hour	-	+	+	+	-

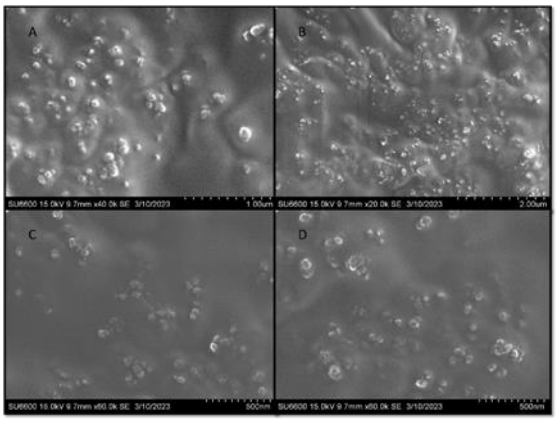

Figure 16. Images of SEM analysis. A) 15.0kV 9.7mm x 40.0k. 1µm. B) 15.0kV 9.7mm x 20.0k. 2µm. C) 15.0kV 9.7mm x 60.0k. 500nm. D) 15.0kV 9.7mm x 60.0k. 500nm.

According to the results, AgNPs were spherical and about 50nm in size

3.4. Antioxidant Assay

3.4.1. Total Flavonoid Content

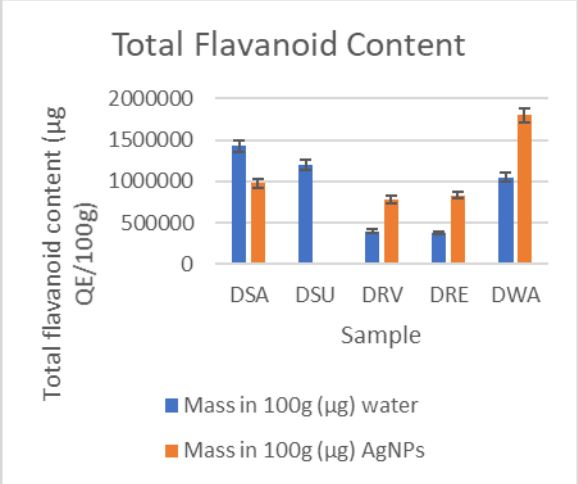

Figure 17. Total Flavonoid Content.

The TFC of DRV, DRE, and DWA AgNPs was higher compared to the water extracts of them.

3.4.2. Total Phenolic Content

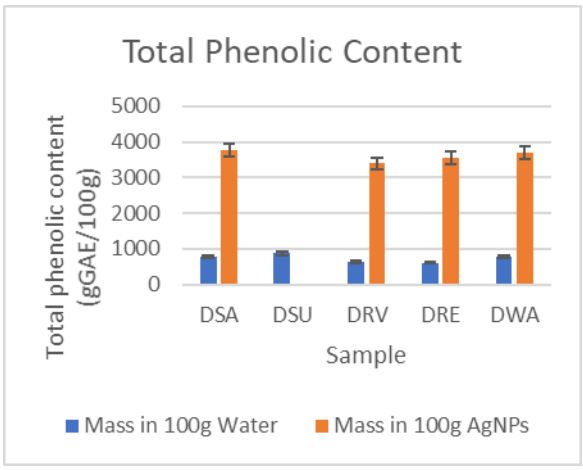

Figure 18. Total Phenolic Content

The total phenolic content of AgNPs was higher compared to the water extracts of them.

3.4.3.Total Antioxidant Capacity

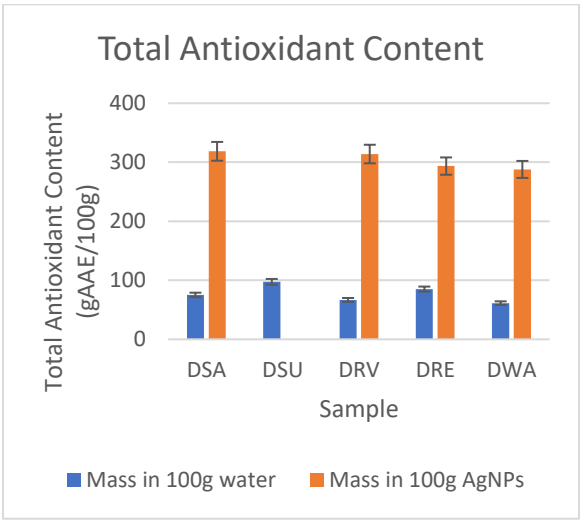

Figure 19. Total Antioxidant Content

The total antioxidant content of AgNPs was higher compared to the water extracts of them.

3.4.4. 2, 2-Diphenyl-1-picrylhydrazyl (DPPH) Scavenging Activity

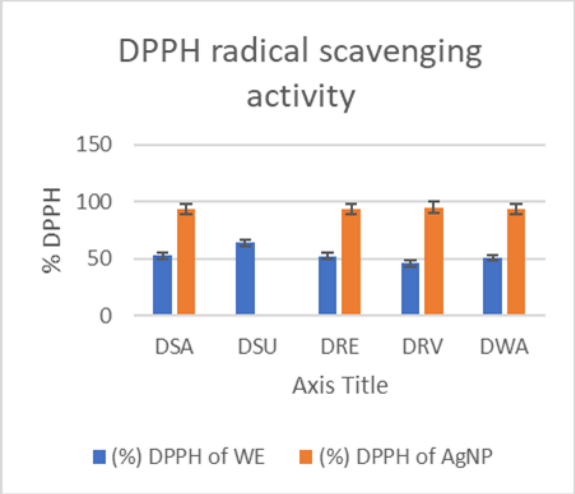

Figure 20. DPPH radical scavenging activity.

The DPPH percentage activity of AgNPs was higher compared to the water extracts.

3.5. Photocatalytic Activity under Sunlight

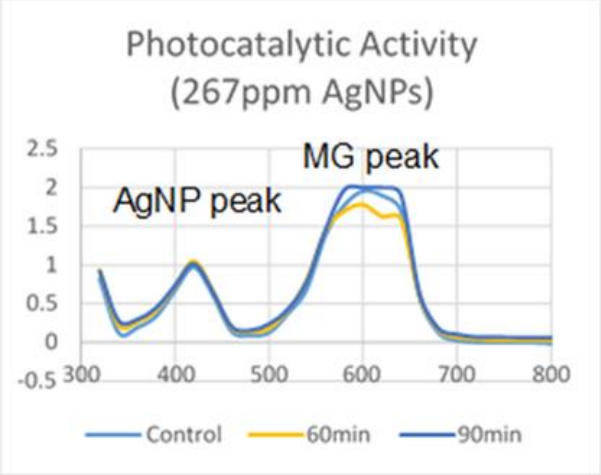

Figure 21. Photocatalytic activity (267ppm AgNP without $NaBH_4$).

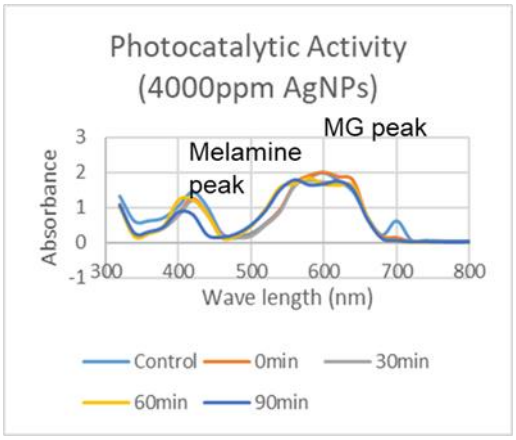

Figure 22. Photocatalytic activity (4000ppm AgNP without $NaBH_4$).

No degradation was observed even after 90 mins (Figure 21 and 22)

Figure 23. Color change of 267ppm AgNP after adding $NaBH_4$

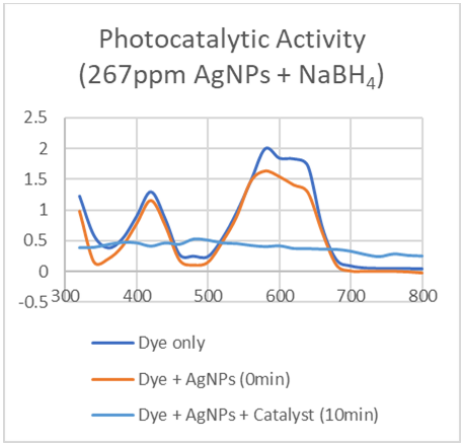

Figure 24. Photocatalytic activity (267ppm AgNP with $NaBH_4$)

Malachite green was degraded in 10minutes after adding $NaBH_4$

Figure 25. Color change of 4000ppm AgNP after adding $NaBH_4$.

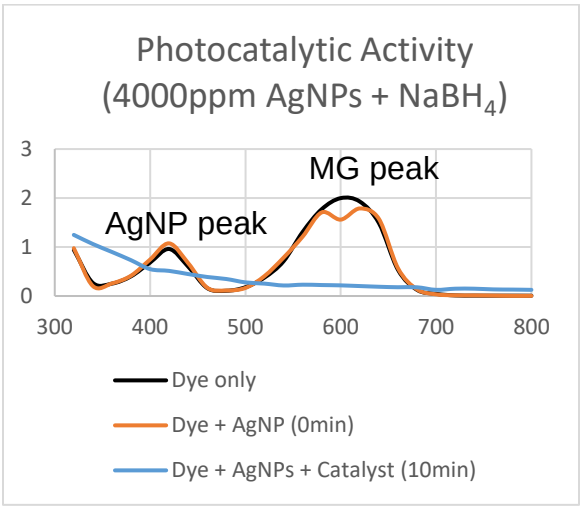

Figure 26. Photocatalytic activity (4000ppm AgNP + $NaBH_4$)

Malachite green was degraded in 10minutes after adding $NaBH_4$.

3.6. Melamine Detection

3.6.1. Melamine detection using DRE AgNPs.

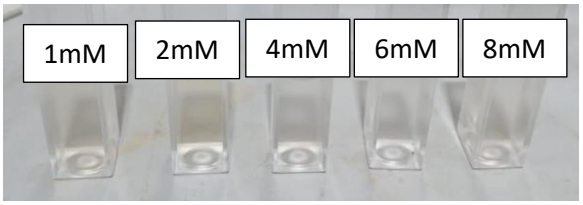

Figure 27. Melamine + DRE AgNPs (0minutes).

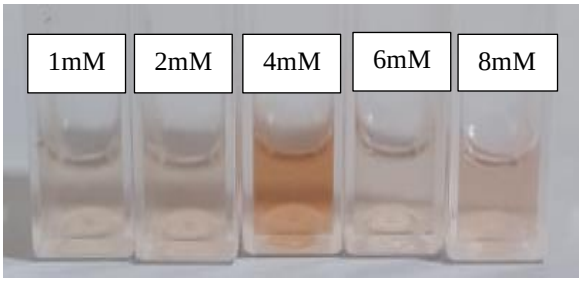

Figure 28. Melamine + DRE AgNPs (40minutes).

As shown in the figures the color change was observed after 40 minutes.

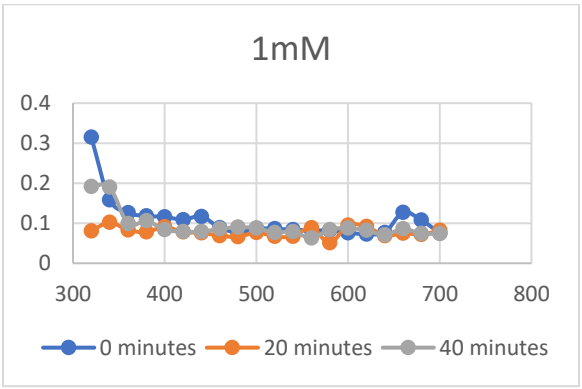

Figure 29. 1mM melamine detection using DRE AgNPs.

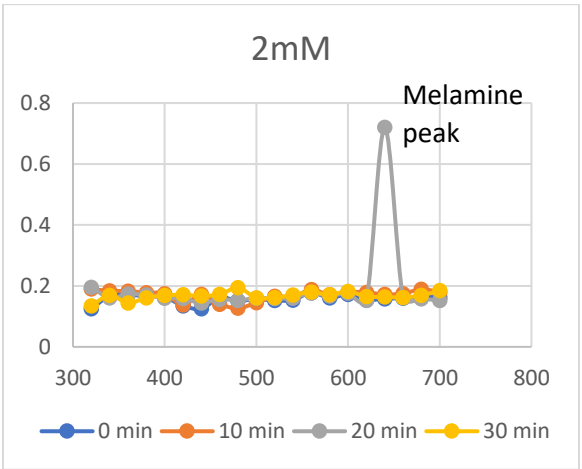

Figure 30. 2mM melamine detection using DRE AgNPs.

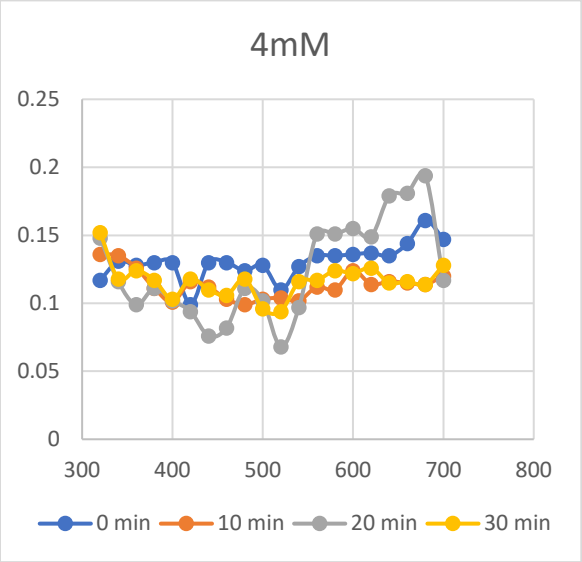

Figure 31. 4mM melamine detection using DRE AgNPs.

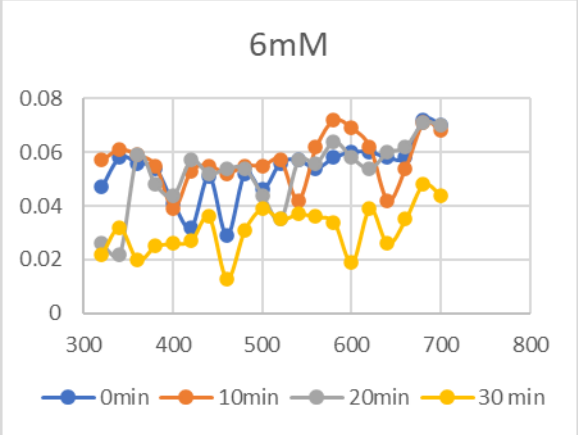

Figure 32. 6mM melamine detection using DRE AgNPs.

Melamine was detected in 2mM melamine solution.

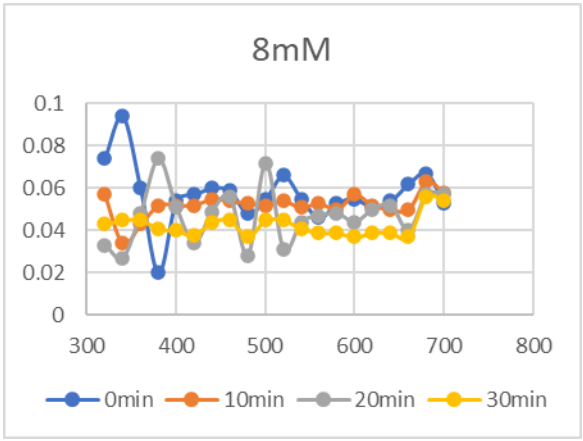

Figure 33: 8mM melamine detection using DRE AgNPs.

3.6.2. Melamine detection on spike milk.

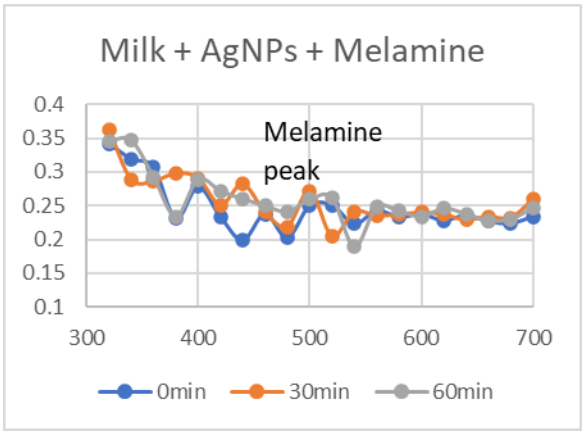

Figure 34. Melamine detection in milk using DRE AgNPs.

Figure 35. Melamine detection in milk using DRE AgNPs (0 minutes).

Melamine was detected at 520nm and there was a slight color change.

Antibacterial Activity

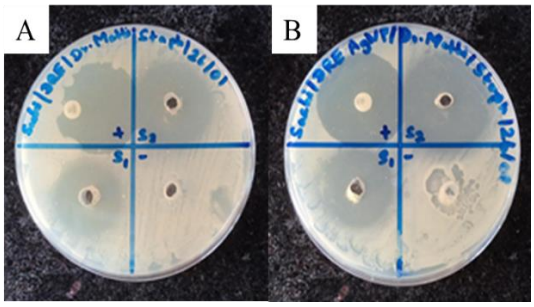

Figure 36. ZOI of *S. aureus*. A) WE and B) DRE AgNPs.

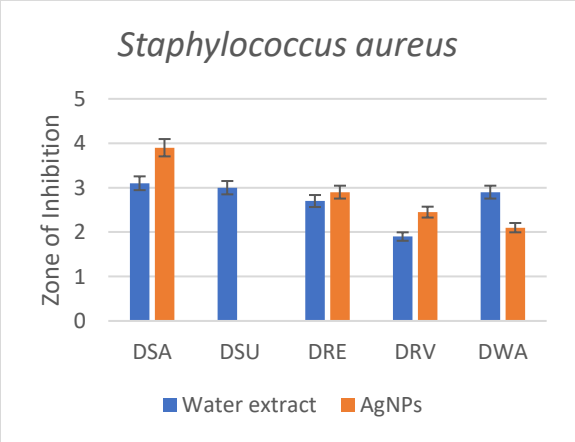

Figure 37. ZOI of S. *aureus*

DSA AgNPs showed the highest ZOI.

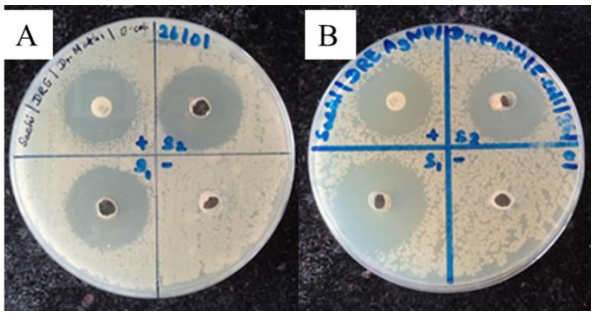

Figure 38. ZOI of *E.coli*. A) WE and B) DRE AgNPs.

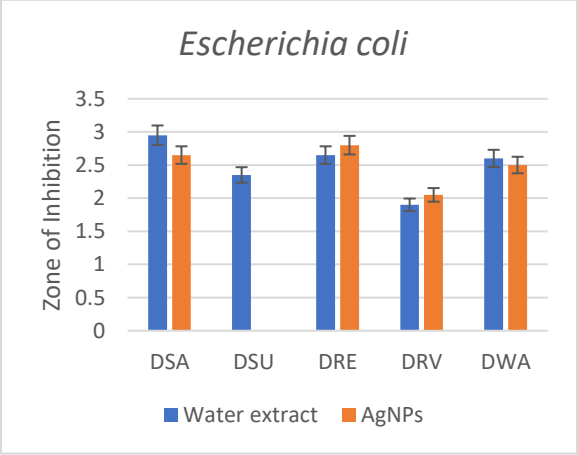

Figure 39. ZOI of *E.coli*.

DRE AgNPs showed the highest ZOI.

According to the ONE-way ANOVA, the p-value of *E.coli* was higher than *S. aureus* and the F-value of *S. aureus* was higher than *E.coli*.

4. Discussion

In this study, nanoparticles were synthesized using *Dracaena* leaf varieties with the biological method which uses nontoxic and environmentally benign materials in conjunction with green technology and is therefore eco-friendly and more acceptable than traditional methods.[30] Plant-based materials seem to be the best candidates and they are suitable for large-scale 'biosynthesis' of nanoparticles. The key active agent in some of these syntheses is believed to be polyphenols which are antioxidants. These

antioxidants have a wide range of biological effects, such as anti-inflammatory, antibacterial, antiviral, anti-aging, and anticancer.[24] In this study, water was used as the green extraction solvent due to its non-inflammability, nontoxicity, and opportunities for clean processing and pollution prevention.[25] Greener synthesis of nanoparticles provides advancement over other methods as it is simple, cost-effective, and relatively reproducible and often results in more stable materials.[26]

The presence of phytochemicals (proteins, carbohydrates, saponins, tannins, phenols, flavonoids, and steroids) in the *Dracaena* samples was confirmed by phytochemical analysis (Table 01).

According to the results, the synthesis of AgNPs was confirmed by the color change observed (Figure 01). This is due to the excitation of the SPR and SPR band which both play an important role in the confirmation of AgNP formation.[27] The peaks were observed at 400nm from DSA, DRE, DRV, and DWA samples except for the DSU sample. This can be due to the slow formation and incomplete bioreduction.[28] During this process, phytochemicals and enzymes present in the plant extract, reduce Ag^{+} to Ag^{0}. Unstable Ag^{0} will be stabilized by the active compounds present in the plant extract.[29] AgNPs synthesized at 90ºC in 15 minutes were taken as the optimized samples. Temperature is an important parameter that affects the synthesis of nanoparticles using all three methods (physical, chemical, and biological).[30] In most cases, the synthesis of nanoparticles using green technology requires temperatures less than 100°C or ambient temperature.[31]

SEM analysis which provides high-resolution imaging revealed the morphology of AgNPs as spherical and 50nm in size.

The measurement of the band gap of materials is important in the semiconductor, nanomaterial, and solar industries. The term “band gap” refers to the energy difference between the top of the valence band to the bottom of the conduction band, electrons are able to jump from one band to another. In order for an electron to jump from a valence band to a conduction band, it requires a specific minimum amount of energy for the transition, the band gap energy. The band gap energy of insulators is large (> 4eV), but lower for semiconductors (< 3eV).[32] According to the synthesized *Dracaena* AgNPs, all the peaks were observed at 400nm and 3.10eV resulted as the energy band gap of all AgNPs. It was calculated using the following equation (Figure 40).

The obtained band gap energy shows that all the AgNPs are semiconductors.

The mechanism of antioxidant actions involved either hydrogen atom transfer, transfer of a single electron, sequential proton loss electron transfer,

$$\boldsymbol{E = h \times \frac{C}{\lambda}}$$

h	Planks constant (6.626×10^{-34} Joules sec)
C	Speed of light
λ	Wavelength shown in the UV visible spectrometer

Figure 40. Planks Equation.

and chelation of transition metals.[33] Polyphenols are the natural antioxidants present in plants.[24] Phenolic compounds act as an antioxidant by reacting with a variety of free radicals.[33] Flavonoids act as antioxidants due to their strong capacity to donate electrons or hydrogen atoms.[34] However, the studies confirmed the presence of antioxidants in *Dracaena* samples.

The TFC was determined using the Aluminium chloride colorimetric method. The C-4 keto group and either the C-3 or C-5 hydroxyl group of flavones and flavonols create acid-stable

complexes with aluminium chloride, according to the basic idea behind the method mentioned. Additionally, it combines with the ortho-dihydroxyl groups on the A or B ring of flavonoids to create complexes that are acid labile.[35] According to the results at 415nm, the highest flavonoid content was observed in DWA AgNPs and the lowest was observed in DRV AgNPs (Figure 4). Similar findings have been found by Vasudevan, Kumar and Sabu in 2019.[10] According to the ONE-way ANOVA, the p-value was 0.45 ($p>0.05$) which means there is no statistical significance. F-value was 0.6 and the F-crit value was 5.99 ($F<Fcrit$) which means there is no significant difference between samples.

The Folin-Ciocalteu reagent technique was used to calculate the TPC. The creation of complex blue compounds that can be detected at a wavelength of 750 nm is the fundamental idea behind this technique. In order to convert the heteropoly acid (phosphomolybdate-phosphotungstate) present in the Folin-Ciocalteau reagent into a molybdenum-tungsten compound, the phenol or phenolic-hydroxy groups in the reagent will be oxidized.[36] According to the results, the highest phenolic content was observed in DSA AgNPs and the lowest was observed in DRV AgNPs (Figure 05). Similar findings have been found by Vasudevan, Kumar and Sabu in 2019.[10] According to the ONE- way ANOVA, the p-value was 7.28E-08 ($p<0.05$) which means there is statistical significance. F-value was 969.89 and the F-crit value was 5.99 ($F>Fcrit$) which means there is a significant difference between samples.

The TAC was determined using the phosphomolybdenum method. This is based on the reduction of Mo (VI) to Mo (V) by the extract and subsequent formation of a green phosphate/Mo (V) complex at acid.[10] According to the results, the highest antioxidant content was observed in DSA AgNPs and the lowest was observed in DWA AgNPs (Figure 06). A similar finding has been found by Li, Chen and Xiao in 2021.[37] According to the ONE-way ANOVA, the p-value was 2.53E-07 ($p<0.05$) which means there is statistical significance. F-value was 638.38 and the F-crit value was 5.99 ($F>Fcrit$) which means there is a significant difference between samples.

The correlation was carried out to figure out the contribution of phenols and flavonoids in the total of antioxidants.

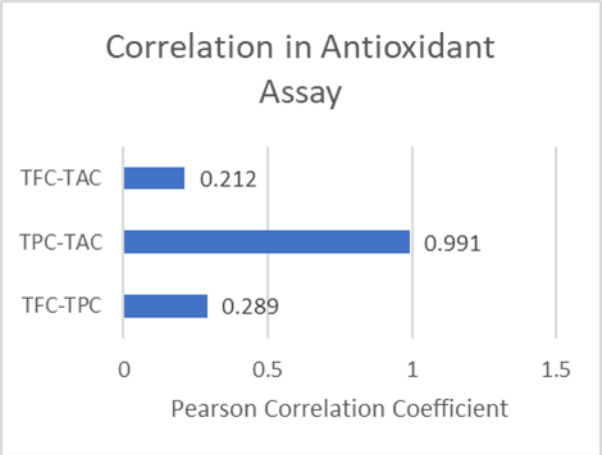

Figure 41. Pearson Correlation Coefficient.

A weak correlation was indicated between TFC and TAC assay which is 0.212 when compared to the correlation between TPC and TAC assay which is 0.991 (Figure 41). Therefore, TFC-TAC is weakly correlated, TPC-TAC is strongly correlated and TFC-TPC is weakly correlated. This can be due to the different antioxidant activities of different phenolic, and flavonoid structures present in the sample.[38] A similar finding has been found by Vasudevan, Kumar and Sabu in 2019.[10]

The radical scavenging activity of the water extracts and AgNPs was determined by using DPPH radical scavenging activity. During this assay, violet color DPPH solution is reduced to a yellow-colored product, diphenylpicryl hydrazine, by the addition of the extract in a concentration-dependent manner.[29] According to the results, the highest observed was DRV AgNPs and the lowest was observed in DSA AgNPs (Figure 20). A similar finding has been found by Tyagi *et al*. in 2021.[39]

AgNPs have been imposed as an excellent antimicrobial agent being able to combat bacteria in vitro and in vivo causing infections. The antibacterial capacity of AgNPs covers Gram-negative and Gram-positive bacteria, including multidrug-resistant strains.[40] The death of bacteria may be attributed to the silver nanoparticles' ability to continuously discharge silver ions. The bacterial envelope may be damaged as a result of the adhering ions increasing the cytoplasmic membrane's permeability. Respiratory enzymes may be inactivated following the import of free silver ions into cells, leading to the formation of reactive oxygen species but not adenosine triphosphate. Cell membrane breakdown and DNA alteration can both be triggered by reactive oxygen species. The toxicity of silver, including nanoparticles of silver, to humans, is generally low.[41]

According to the results, ZOI for *S. aureus* was shown higher in the DSA, DRE, and DRV AgNPs than in the water extracts of them, and ZOI for against *E. coli* was shown in the DRE and DRV AgNPs than in the water extracts of them. This can be due to the small size with the large surface area of AgNPs can be attached to the cell membrane or break through it.[42] Similar findings have been found by Palanivelu *et al*. in 2015.[43] According to the ONE- way ANOVA, in *S. aureus*, p-value was 0.79 ($p>0.05$) which means there is no statistical significance. F-value was 0.08 and the F-crit value was 5.59 ($F<Fcrit$) which means there is no significant difference between samples. In *E.coli*, p-value was 0.97 ($p>0.05$) which means there is no statistical significance. F-value was 0.002 and the F-crit value was 5.59 ($F<Fcrit$) which means there is no significant difference between samples.

Photocatalytic activities harness light energy to excite the photo-induced electrons.[44] The dye must first bind to the surface of the NPs in order to generate an electron-hole when exposed to sunlight. Oxygen and the superoxide anionic radical react with the electron in the conductance band. A hydrogen ion and a hydroxyl anion are created when the hole in the valence band interacts with water molecules. Another hole produces hydroxyl radicals when it interacts with water molecules at the same time. In parallel, dye is triggered by sunlight absorption and simultaneously releases electrons to make dye while producing dye. When the dye combines with two extremely unstable species, hydroxyl radicals and superoxide anionic radicals, it creates CO_2 and water as breakdown products (Figure 42).[45]

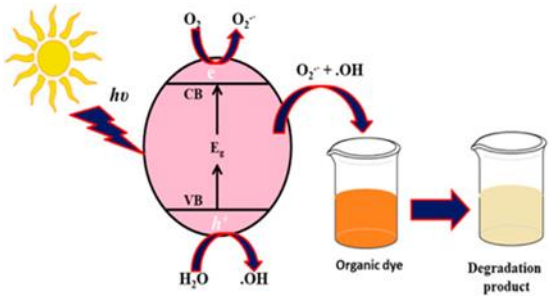

Figure 42. Mechanism of Photocatalytic activity.[4]

In this study, the azo dye used was Malachite Green in order to degrade and achieve complete mineralization.[46] The degradation process of MG confirmed the pseudo-first-order kinetics as shown below (Figure 43).[44]

$$\ln (C_0/C_t) = kt$$

C_0	The initial concentrations
C_t	The concentration at time t
k	Pseudo-first-order rate coefficients
t	Time

Figure 43. Pseudo first-order kinetics equation.

The photodegradation of MG dye assessed the photocatalysts' performance under UV irradiation. The catalyst used was $NaBH_4$ to give more degradation. The role of $NaBH_4$ is to produce $BH4^{-1}$ which acts as an electron relay to provide AgNPs with more electrons to produce more radicles which is why AgNPs have been reported to degrade organic dyes in a short period.[47]

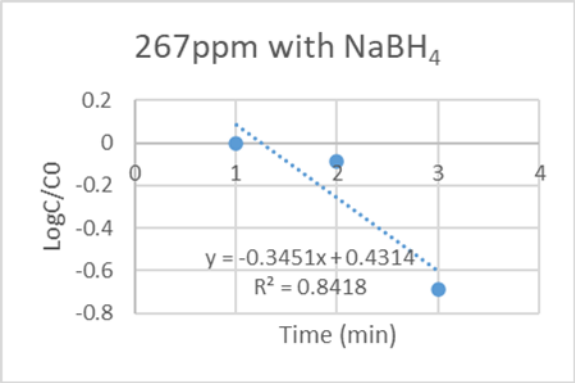

Figure 44. Rate Constant (267ppm AgNPs + NaBH4).

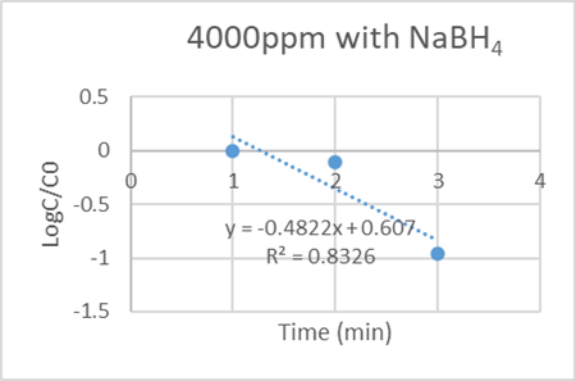

Figure 45. Rate Constant (4000ppm AgNPs + NaBH4)

According to the results, the color change was observed from dark blue to colorless after the addition of $NaBH_4$ (Figure 23 and 25). In 267ppm AgNPs, the MG absorption peak at 580nm was shown to be decreasing with time. The rate constant for 267ppm showed 0.3451. The degradation was completed in 10 minutes. In 4000 ppm, the MG absorption peak at 600 nm was also shown to be decreasing with time and the degradation was completed in 10 minutes. The rate constant for 4000 ppm showed 0.4822. It can be concluded that 4000 ppm can degrade the dye more efficiently.

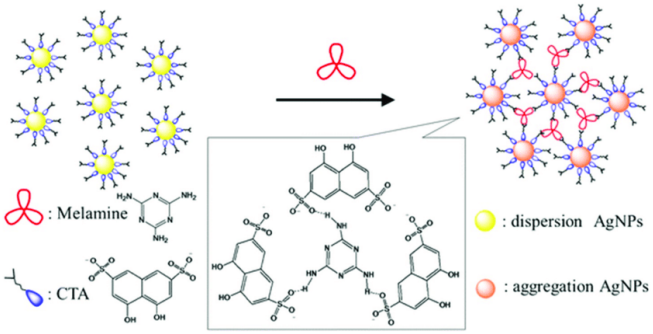

Figure 46. Mechanism of Melamine detection.[48]

Nanotechnology is used in melamine detection. Melamine causes the aggregation of AgNPs and the yellow color changes to red. Change in the color of AgNPs is the basis of the colorimetric detection method (Figure 46).[36]

According to the results, color change was observed within 40minutes in 2mM melamine concentrations (Figure 27, 28). The lowest melamine concentration (2mM) was used for the melamine detection in milk and a color change was observed (Figure 35).

Conclusion

Five *Dracaena* plant varieties were used in order to synthesize AgNPs and the optimized conditions were 90ºC for 15minutes. Synthesized AgNPs were spherical and 50nm in size according to SEM analysis. According to the antioxidant assay results, AgNPs showed a higher antioxidant activity than the water extracts of

them. Furthermore, high antimicrobial activity was shown by the AgNPs against *E. coli* compared to *S. aureus* which means that the AgNPs' effectiveness against gram-negative bacteria is higher. The photocatalytic activity was more efficient in 4000ppm AgNPs compared to 267ppm AgNPs and the degradation of the dye was faster after the addition of $NaBH_4$. Melamine was detected using DRE AgNPs in both 2mM melamine solution and spike milk. AgNPs play major roles in anti-inflammatory, anti-cancer, anti-proliferative, and biosensing and imaging processes. Cardiovascular, and neurological disorders are also treated using AgNPs.

Acknowledgements

Authors thank BMS for funding and SLINTEC for SEM analysis.

References

1. N. Sanchooli, S. Saeidi, H.K. Barani and E. Sanchooli, *Iranian Journal of Microbiology*, 2018;**10**(6);400-408.
2. X.F. Zhang, Liu ZG, Shen W and Gurunathan S. *International Journal of Molecular Science*, 2016; **17**(9);1534.
3. M.F.A. Hakkani. *Applied Sciences*. 2020;**2**(3).
4. M. Nasrollahzadeh, S.M. Sajadi, M. Sajjadi and Z. Issaabadi. *Interface Science and Technology*, 2019; **28**;113-143.
5. J. Singh, T. Dutta, K.H. Kim, M. Rawat, P. Samddar and P. Kumar. *Journal of Nanobiotechnology*, 2018; **16**;84.
6. S.P. Goutam, G. Saxena, D. Roy and A.K. Yadav. *Industrial Waste and Its Management*. 2019;349-379.
7. S. Iravani, H. Korbekandi, S.V. Mirmohammadi and B. Zolfaghari. *Research in Pharmaceutical Sciences*, 2014;**9**(6);385-406.
8. C. Dhand, N. Dwivedi, X.J. Loh, A.N.J. Ying, N.K. Verma, R.W. Beuerman, R. Lakshminarayanan and S. Ramakrishna. *Royal Society of Chemistry.* 2015;**5**; 105003– 105037.
9. S. Zafar and A. Zafar. *The Open Biotechnology Journal*. 2019;**13**;37-46.
10. K. Vasudevan, R.S. Kumar and M.C. Sabu, *Journal of Pharmaceutical Science and Research*. 2019;**11**(5); 1874–1879.
11. S. Knapp. Oxidative stress. *Biology Dictionary*. 2020.
12. S. Irina, A. Kutsak, L. Gordienko, V. Bulanov, T. Hryshyna, V. Zarytska, O. Plakhotnik, I. Semeniv, A. Kotuza, I. Zazirnyi, Y. Kmetyuk and R. Kovtun. etric *French-Ukrainian Journal of Chemistry*, 2020;**8**(1).
13. S.C. Lourenco, M.M. Martins, V.D. Alves, *Molecules*. 2019;**24**(22);4132.
14. ProFlowers. How to care for Dracaena: growing information and tips. 2017.
15. S.B. Kedare and R.P. Singh, *Journal of Food Science and Technology.* 2011;**48**(4);412 – 422.
16. A.S. Jain, P.S. Pawar, A. Sarkar and V. Junnuthula. *International Journal of Molecular Sciences*, 2021;**22**(21);11993.
17. A. Paul and M. Kurian. *Chapter 26 – catalytic applications of carbon dots. Carbon Dots in Analytical Chemistry*, 2023;337 – 344.
18. P. Rani, V. Kumar, P.P. Singh, A.S. Matharu, W. Zhang, K.H. Kim, J. Singh and M. Rawat, *Environmental Internationa,*. 2020;143.
19. S. Marimuthu, A.J. Antonisamy, S. Malayandi, K. Rajendran, P.C. Tsai, A. Pugazhendhi and V.K. Ponnusamy. *Journal of Photochemistry and Photobiology B: Biology*, 2020;**205**;111823.
20. C.G. Skinner, J.D. Thomas and J.D. Osterloh. *Journal of Medical Toxicology*, 2010;**6**(1);50-55.
21. Jigyasa and J.K Rajputh. *Biosensors and Bioelectronics*, 2018;**120**;153-159.
22. K. Ramalingam, T. Devasena, B. Senthil, R. Kalpana and R. Jayavel. *Measurement & Technology*, 2017; **11**(2);171–178.
23. S. Shankar, S. Settu, G. Segaran, V.S. Dhevi and L. Ravi. *Biotechnology Research and Innovation*. 2018; **1**(2);1-8.
24. D.P. Xu, Y. Li, X. Meng, T. Zhou, Y. Zhou, J. Zheng, J.J. Zhang and H.B. Li, *International Journal of Molecular Sciences*, 2017;**18**(1);96.
25. A. Filly, A.S.F. Tixier, C. Louis, X. Fernandez and F. Chemat. *Comptes Rendus Chimie*, 2016;**19**(6);707–717.
26. O.V. Kharissova, H.V.R. Dias, B.I. Kharisov, B.O. Pérez and V.M.J. Pérez, *Trends in Biotechnology*, 2013;**31**(4);240–248.
27. M. Vanjana, R. Shanmugam, K. Paulkumar and G. Gnanajobitha. *Advances in Applied Science Research*, 2013, **4**(4), 50-55.
28. A.O. Dada, F.A. Adekola, F.E. Dada, A.T. Adelani-Akande, M.O. Bello, C.R. Okonkwo, A.A. Inyinbor, A.P. Oluyori, O. Adeniyi, K.O. Ajanaku, C.O. Oluwaseun and C.O. Adetunji. *Heliyon*, 2019;5.
29. H.B.H. Rahuman, R. Dhandapani, S. Narayanan, V. Palanivel, R. Paramasivam, R. Subbarayalu, S. Thangavelu and S. Muthupandian. *IET Nanobiotechnology*, 2022;**16**(4);115–144.
30. J.K. Patra, K.H. Baek. *Journal of Nanomaterials*, 2014;1–12.
31. A. Rai, A. Singh, A. Ahmad and M. Sastry. *Langmuir*, 2006;**22**(2);736–741.

32. J. Dharma, A. Pisal and C. Shelton. *Application Note*. 2009.
33. A. Zeb. *Journal of Food Biochemistry*. 2020;**44**(9).
34. I. Hernández, L. Alegre, F. Van Breusegem, S. Munné-Bosch. *Trends in Plant Science,* 2009;**14**(3); 125–132.
35. F. Ahmed and M. Iqbal. *Organic and Medicinal Chemistry International Journal,* 2018;**5**(4);107-112.
36. N. Kumar, H. Kumar, B. Mann and R. Seth. *Spectrochimica Acta Part A Molecular and Biomolecular Spectroscopy*. 2015.
37. C. Li, D. Chen and H. Xiao. *Materialstoday Communications*, 2021;26.
38. S. Kaur. *Journal of Microbiology & Experimentation*, 2014;**1**(1).
39. P.K. Tyagi, S. Tyagi, D. Gola, A. Arya, S.A. Ayatollahi, M.M. Alshehri and J.S. Rad. *Journal of Nanomaterials,* 2021.
40. T. Bruna, F.M. Bravo, P. Jara and N. Caro. *International Journal of Molecular Sciences*, 2021;22(13);7202.
41. I.X.Yin, J. Zhang, I.S. Zhao, M.L. Mei, Q. Li and C.H. Chu. *International Journal of Nanomedicine*. 2020;15;2555–2562.
42. A.B.A. Mohammed, M.M.A. Elhamid, M.K.M. Khalil, A.S. Ali and R.N. Abbas. *Environmental Sciences Europe*, 2022;**34**(1).
43. J. Palanivelu, M. Kunjumon, A. Suresh, A. Nair and C. Ramalingam. *Journal of Phamaceutical Science and Research*, 2015;690–695.
44. G.E. Lau, C.A.C. Abdullah, W.A.N.W. Ahmad, S. Assaw and A.L.T. Zheng, *Catalysts*. 2020;**10**(10);1129.
45. P.G. Krishna, P.C. Mishra, M.M. Naika, M. Gadewar, P.P. Ananthaswamy, S. Rao, S.R.B. Prabhu, K.V. Yatish, H.G. Nagendra, M. Moustafa, M.A. Shehri, S.K. Jha, B. Lal and S.M.S. Santhakumari. *Frontiers in Chemistry*, 2022;10.
46. V. Selvaraj, T.S. Karthika, C. Mansiya and M. Alagar. *Journal of Molecular Structure*. 2021;**1224**;129195.
47. R.E. Adam, G. Pozina, M. Willander and O. Nur. *Fundamentals and Applications*, 2018;**32**:11–18.
48. M. Shellaiah, K.W. Sun. *Chemosensor*s, 2019;**7**(1):9.
49. A. Bhattacharya, P. Sood and V Citovsky V. *Molecular plant pathology*. 2010;**11**(5):705–19.
50. Catauro M, Tranquillo E, Poggetto GD, Pasquali M, Era AD, Ciprioti SV. *Materials*, 2018;**11**(12):2364.
51. A.J. Lafta, E.J. Mohammad, and S.H. Kadhim. *International Journal of Chemical Sciences*. 2016;**14**(2);993-1004.
52. D.A.A. Makuasa and P. Ningsih. *Journal of Applied Science Engineering Technology and Education*, 2020;**2**(1):11-17.
53. G. Mountrichas, S. Pispas and E.I. Kamitsos. *The Journal of Physical Chemistry C*. 2014;**118**(39):22754–22759.
54. N. Sadeer, D. Montesano, S. Albrizio, G. Zengin and F. Mahomoodally. *Antioxidants*, 2020;**9**(8);709.
55. L. Shi, W. Zhao, Z. Yang, V. Subbiah, H.AR. Suleria Environmental Science and Pollution Research, 2022;**29**;81112 – 81129.
56. M.R.C. Sytu and D.H. *BioNanoScience*, 2018;**8**:835-844.
57. ProFlowers. How to care for Dracaena: growing information and tips. 2017.
58. F. Mokobi. Scanning electron microscope (SEM)-definition, principle, parts, images. Microbe Notes. 2022.